INVESTIGATION OF DE-HOMOGENIZATION FOR PWR LATTICE CELLS IN DRAGON5

A THESIS SUBMITTED IN PARTIAL FULFILLMENT

OF THE REQUIREMENTS FOR THE AWARD OF THE DEGREE OF

MASTER OF TECHNOLOGY

IN

NUCLEAR SCIENCE AND ENGINEERING

SUBMITTED BY

NIMPHY SARKAR

2K16/NSE/02

UNDER THE GUIDANCE OF

DR. NITIN KUMAR PURI

ASSISTANT PROFESSOR

DEPARTMENT OF APPLIED PHYSICS

DELHI TECHNOLOGICAL UNIVERSITY

SHAHBAD DAULATPUR, MAIN BAWANA ROAD,

DELHI- 110042

CERTIFICATE

DEPARTMENT OF APPLIED PHYSICS

DELHI TECHNOLOGICAL UNIVERSITY

This is to certify that Ms. Nimphy Sarkar, a second-year student of M.Tech., Nuclear Science & Engineering, from Department of Applied Physics, Delhi Technological University, has successfully completed the project work 'INVESTIGATION OF DE-HOMOGENIZATION FOR PWR LATTICE CELLS IN DRAGON5' and has submitted a satisfactory thesis on this volume as per requirement of university which may be accepted for the partial fulfillment of degree of Master of Technology.

Dr. Nitin Kumar Puri

Assistant Professor
Department of Applied Physics
Delhi Technological University

ACKNOWLEDGMENT

I would like to express my sincere appreciation to my supervisor, Dr. Nitin Kumar Puri for his invaluable support, guidance, comments, and suggestions during the course of the project that made it possible. Thank you for the motivation you gave me to finish this work.

I would also like to thank Ms. Archana Sharma from BARC, Mumbai for her guidance and help in different stages of this effort. To her, my gratefulness will always fall short.

I deeply express my sincere thanks to Prof. Suresh C. Sharma, Head of the Department, for allowing me to present this work at the department premises for the partial fulfillment of the requirements leading to the award of M.Tech degree.

Last but not least, I would like to offer my heartiest thanks to my mother for her encouragement and support throughout the different stages of this effort, and to God for always inspiring me in different ways.

ABSTRACT

The objective of this study is to inspect the accuracy of the dehomogenization in the 3 x 3 PWR assembly PWR for homogeneous homogenization and heterogeneous homogenization. Based on the Method of Characteristics, the 2-level computational scheme and subgroup projection method is used with SHEM 361 group energy mesh. In this case, homogeneous geometry and heterogeneous geometry are used. Using the NAP: module, a two-level computational scheme including the core with heterogeneous assemblies are generated. Enrich multi-parameter data structure was obtained to keep the pin wise flux for diffusion calculations with different homogenization options. Using Pin Power Reconstruction, the results for both geometries are compared and discrepancies are calculated. It is showed that heterogeneous geometry gives more accurate and promising results. With the generation of multi-parameter reactor database, it is observed that the computational time is also reduced with Method of Characteristics and the two-level scheme approach.

TABLE OF CONTENTS

LIST OF FIGURES

LIST OF TABLES

LIST OF ACRONYMS

LWR	Light Water Reactor
PWR	Pressurized Water Reactor
BWR	Boiling Water Reactor
PHWR	Pressurized Heavy Water Reactor
ADF	Assembly Discontinuity Factor
CDF	Corner Discontinuity Factor
GET	Generalised Equivalence Theory
GFF	Group Form Function
SHEM	Santamarina-Hfaiedh Energy Mesh
SPH	Superhomogenization
SPM	Subgroup Projection Method
PPR	Pin Power Reconstruction
MOC	Method of Characteristics

CHAPTER 1: INTRODUCTION

Full transport calculations are the keys to the design and operation of a thermal nuclear reactor. However, full transport calculations for the entire core are too complicated to be done in reasonable time. To keep the computational time reasonable, other methods are used to do the neutronics calculations. This is usually done in two steps. The first step is the transport calculations which are done at the assembly level. In this step, large averaged neutronics properties are generated. These homogenized properties are used for the core calculations which is the second step.

In case of Pressurized Water Reactors (PWRs) and Pressurized Heavy Water Reactors (PHWRs), most facets of homogenization methodologies are common. The major drawback of this method is losing the specific aspects at assembly and pin levels. In recent studies by Fliscounakis et al. (2011) and Brosselard et al. (2014), we can capture more precise details by pin power reconstruction method. For homogenized fuel assemblies, this technique can be taken as a de-homogenization method for reactor core computations.

This study is focused on homogenization and de-homogenization techniques for PWRs.

1.1: Neutron Transport Equation

In a nuclear reactor core, the neutron transport equation represents the conduct of neutrons most accurately. The neutron transport equation takes following assumptions.

1. The relativistic effects are neglected. Maximum neutron speeds achieved in a nuclear reactor are less than 1/10th of the speed of light.
2. Only neutron collisions with nuclei are considered. This is done to keep the equation linear. Neutron-neutron collisions are ignored because the neutron density is several orders of magnitude smaller than the atom density of materials in a reactor.
3. The neutron paths between collisions are assumed to be in straight lines.

Equation (1.1) shows the continuous-energy transport equation. For any arbitrary infinitesimal volume, this equation demonstrates the neutron balance equation.

$$\begin{aligned}\frac{\partial n(\vec{r},E,\hat{\Omega},t)}{\partial t} = &-\hat{\Omega}\cdot\nabla\psi(\vec{r},E,\hat{\Omega},t) - \Sigma_t(\vec{r},E,t)\psi(\vec{r},E,\hat{\Omega},t) + \\ &+\int_0^\infty\int_{4\pi}\Sigma_s(\vec{r},E'\rightarrow E,\hat{\Omega}'\rightarrow\hat{\Omega},t)\psi(\vec{r},E',\hat{\Omega}',t)\,d\hat{\Omega}\,dE' + \\ &+\frac{\chi(E)}{4\pi}\int_0^\infty \nu(E')\Sigma_f(\vec{r},E',t)\psi(\vec{r},E',t)\,dE' + S(\vec{r},E,\hat{\Omega},t)\end{aligned} \qquad (1.1)$$

Equation (1.1) is called the integrodifferential form of the transport equation.

This is also called integrodifferential equation because it has a part of the partial differential equation and a part of an integral equation. The left side represents the angular rate of change of angular neutron density with respect to time.

$\psi(\vec{r}, E, \hat{\Omega}, t)$: angular flux as a function of position, energy, solid angle, and time

$\Sigma_t(\vec{r}, E, t)$: macroscopic total removal cross-section

$\Sigma_s(\vec{r}, E' \rightarrow E, \hat{\Omega}' \rightarrow \Omega, t)$: scattering downward into the energy removal cross-section

$\chi(E)$: normalized fission neutron energy distribution

$\nu(E')$: total neutron yield as a function of energy

$\Sigma_f(\vec{r}, E', t)$: macroscopic fission cross-section

$\psi(\vec{r}, E', t)$: total neutron flux

Fission reaction is independent of the direction of neutrons in the target volume. Thus, there is no argument of solid angle in the above flux function.

Below, the terms of the right side of equations (1.1) are explained below in separate terms. The first term denotes the loss of neutrons due to leakage from an infinitesimal volume.

Loss by leakage : $\hat{\Omega} \cdot \nabla \psi(\vec{r}, E, \hat{\Omega}, t)$ (1.2)

Second term on right side in the equation (1.1) is shown separately in equation (1.3) below. This term referred to the total removal rate. It denotes neutron losses due to nuclear interactions (such as absorption and scattering).

Total removal rate = $\Sigma_t(\vec{r},E,t)\psi(\vec{r},E,\hat{\Omega},t)$ (1.3)

In Equation (1.4), neutrons gain due to scattering interactions of neutrons in an infinitesimal volume is represented.

Neutrons gain due to scattering:

$$\int_0^{\infty}\int_{4\pi}\Sigma_s(\vec{r},E'\rightarrow E,\hat{\Omega}',\hat{\Omega},t)\psi(\vec{r},E',\hat{\Omega},t)\,d\hat{\Omega}\,dE' \quad (1.4)$$

Equation (1.5) represents the neutron generation from fission reactions.

Neutrons generated from fission:

$$\frac{\chi(E)}{4\pi}\int_0^{\infty}\nu(E')\Sigma_f(\vec{r},E',t)\psi(\vec{r},E',t)\,dE' \quad (1.5)$$

Finally, $s(\vec{r},E,\hat{\Omega},t)$ in above equation denotes an external (independent of the flux level) neutron source.

The leakage term (1.2) includes the gradient of the angular flux. The scattering term shown in equation (1.4) has two integrals: one over the solid angle and another over the energy spectrum. The fission

neutrons source term shown in equation (1.5) has one integral over the energy range. All these constitute a complex integrodifferential form (equation 1.1) of the neutron transport equation. While considering the steady-state case, some fundamental problems associated with the reactor physics can be solved.

For these time-independent problems, simplification of the time-independent neutron balance equation leads to form equation (1.6).

$$\hat{\Omega}\cdot\nabla\psi(\vec{r},E,\hat{\Omega})+\Sigma_t(\vec{r},E)\psi(\vec{r},E,\hat{\Omega})=\int_0^{\infty}\int_{4\pi}\Sigma_s(\vec{r},E\rightarrow E,\hat{\Omega}'\rightarrow\hat{\Omega})\psi(\vec{r},E',\hat{\Omega}')d\hat{\Omega}dE' + \frac{1}{k}\frac{\chi(E)}{4\pi}\int_0^{\infty}\nu(E')\Sigma_f(\vec{r},E')\psi(\vec{r},E')dE' \tag{1.6}$$

In above equation (1.6), the production term is divided by constant k (Effective Multiplication Constant) in order to make the production rate and the loss rate equal. Moreover, all nuclear reactions are dependent on the neutron's energy involved in the interactions. For numerical computations, neutron energy ranges is broken into multiple energy groups through a process called energy discretization. Equation (1.7) represents the multi-group neutron balance transport equation.

$$\nabla\cdot[\hat{\Omega}\psi_g(\vec{r},\hat{\Omega})]+\Sigma_{tg}(\vec{r},\hat{\Omega})\psi_g(\psi,\hat{\Omega})=\sum_{g'}\int_{\Omega}\Sigma_{(g'\rightarrow g\hat{\Omega}'\rightarrow\hat{\Omega})}(\vec{r})\psi_{(g')}(\vec{r},\hat{\Omega})d\hat{\Omega} + \frac{1}{k}\frac{\chi_g}{4\pi}\sum_{g'}\int_{\Omega'}\Sigma_{(fg')}(\vec{r})\psi_{(g')}(\vec{r},\hat{\Omega}')d\Omega' \tag{1.7}$$

In equation (1.7),

$\psi_g(\vec{r},\hat{\Omega})$: condensed flux in group g

$\Sigma_{tg}(\vec{r},\hat{\Omega})$: total removal cross-section from group g

$\Sigma_{(g'\to g,\hat{\Omega}'\to\hat{\Omega})}(\vec{r})$: scattering cross-section

Furthermore, the neutron current can be defined as,

$$\vec{J_g}(\vec{r})=\int_{\Omega}\hat{\Omega}\,\psi_g(\vec{r},\hat{\Omega}')\,d\Omega \tag{1.8}$$

Reaction rates are not dependent on the incident neutron flux's direction. Thus, defining the integral group flux as

$$\phi_g(\vec{r})=\int_{\Omega}\psi_g(\vec{r},\hat{\Omega})\,d\Omega \tag{1.9}$$

In the first leakage component after taking the divergence operator outside, the product term of the solid angle and the group flux can be simplified by substituting it with the current term as per equation (1.8). Moreover, the flux appearing in the source terms can be substituted by equation (1.9). Equation (1.10) represents the multi-group neutron balance equation with the current and integral flux in the source term.

$$\nabla\cdot\overrightarrow{J_g(\vec{r})}+\Sigma_{tg}(\vec{r})\phi(\vec{r})=\sum_{g'}\Sigma_{(g'\to g,\hat{\Omega}'\to\hat{\Omega})}(\vec{r})\phi_{(g')}(\vec{r})+\frac{\chi_g}{k}\sum_{g'}\Sigma_{(fg')}(\vec{r})\phi_{(g')}(\vec{r}) \tag{1.10}$$

From equation (1.10), we can see that finding the solution for the steady-state transport equation (1.10) is a challenging computational

task for full nuclear reactor core. After discretization of various variables, solving the neutron balance equation becomes very complicated. Furthermore, the number of unknowns will only increase linearly with the number of groups. It will also quadratically rise with the number of dimensions from the equation (1.10). The number of unknowns only grows for the larger geometries. This further complicates the neutron balance equation. Therefore, the problem is divided into two parts to make the computation simple and decrease the computation time. First part is to solve the complex neutron balance equation at the lattice cell level. Then, homogenized properties are generated. To find the power distribution of the whole core, these properties are used in the diffusion equation which is the simpler approximation of the neutron transport equation.

1.2: Neutron Diffusion Equation

The simple approximation of the neutron transport equation is done by diffusion theory model. The neutron diffusion equation has a simpler structure which is achieved by using Fick's law. The neutron current is approximated. According to Fick's law, there is a guided flow of neutrons from higher region to lower region.

$$\overline{J}_g = -D_g \nabla \phi_g \tag{1.11}$$

where,

$\vec{J}_g$: group neutron current

ϕ_g : integral neutron flux

D_g : diffusion coefficient of condensed energy group

In equation (1.11), negative sign denotes the reverse orientation of gradient operator on the group flux ϕ_g .

From equation (1.10) and (1.11), the multi-group diffusion equation is derived as shown in equation (1.12).

$$\nabla\cdot[-D_g(r)\nabla\phi_g(r)]+\Sigma_{tg}(r)\phi_g(r)=\sum_{g'}\Sigma_{(g'\to g)}(r)\phi_{(g')}+\frac{\chi}{k}\sum_{g'}\Sigma_{(fg')}(r)\phi_{(g')}(r) \tag{1.12}$$

$$-\nabla[D_g(r)\nabla\phi_g(r)]+\Sigma_{ag}(r)\phi_g(r)+\Sigma_{(s^g_{loss})}(r)\phi_g(r)=\sum_{g'}\Sigma_{(g'\to g)}(r)\phi_{(g')}+\frac{\chi}{k}\sum_{g'}\Sigma_{(fg')}(r)\phi_g(r) \tag{1.13}$$

Equation (1.13) represents the multi-group diffusion equation used for the computation of entire core.

In equation (1.13), the total cross-section Σ_{tg} decomposes to absorption cross-section Σ_{ag} and scatting cross-section (loss due to scattering of neutron over condensed energy group g) $\Sigma(s^g_{loss})$.

For reactor core calculations, two energy group are most often used: a fast energy group (1 keV to 10 MeV) and a slow energy group (0.025 keV to 1 keV). In reactor operations, thermal neutrons (0.025

eV to 1 eV) play an important role. Thermal neutrons are the cardinal for fission. Thermal neutrons are in equilibrium with their ambient energy/temperature. Neutrons from the thermal group are lost to capture, leakage, and up-scattering (due to target-nuclei vibrations). However, fast neutrons are lost due to leakage, resonance capture, and down scattering. Equation (1.13) can be written for the fast group (equation 1.14) and the thermal group (equation 1.15).

$$\Sigma_{a1}(r)\phi_1(r)+\Sigma_{12}(r)\phi_1(r)=\frac{1}{k}(\nu_1\Sigma_{f1}(r)\phi_1(r)+\nu_2\Sigma_{f2}(r)\phi_2(r)) + \Sigma_{21}(r)\phi_2(r)+\nabla(D_1(r)\nabla\phi_1(r)) \quad (1.14)$$

$$\Sigma_{21}(r)\phi_2(r)+\Sigma_{a2}(r)\phi_2(r)=\Sigma_{12}(r)\phi_1(r)+\nabla(D_2(r)\nabla\phi_2(r)) \quad (1.15)$$

ϕ_1 : flux (fast group)

ϕ_2 : flux (thermal group)

Σ_{a1} : absorption cross-section (fast group)

Σ_{a2} : absorption cross-section (thermal group)

Σ_{12} : scattering downward of the cross-section from fast group to thermal group

Σ_{21} : scattering upward from thermal group to fast group

ν_1 : average total neutron yield (fast group)

ν_2 : average total neutron yield (thermal group)

Σ_{f1} : fission cross-section (fast group)

Σ_{f2} : fission cross-section (thermal group)

D_1 : diffusion coefficient for the fast group

D_2 : diffusion coefficient for the thermal group

All the cross-sections used in equation (1.14) and (1.15) are homogenized. k is called the multiplication constant. It is the proportionality of the neutron production rate to the neutron loss rate. For finite geometry, it is k_{eff}. For infinite geometry, it is k_{∞}.

The next section gives a brief outline of the thesis.

1.3: Thesis Outline

This thesis comprised of seven chapters including this chapter. A brief description of the content of each chapter is presented in this section.

Chapter 1: Introduction

This chapter contains a description of the type of calculations used for nuclear power plant design and operations, an explanation of neutron transport equation, neutron diffusion equation and Thesis outline.

Chapter 2: Problem Statement

This chapter contains a description of typical PWR lattice cell, the standard homogenization (SH) method, and problems with the SH methodology.

Chapter 3: Progress to date in LWR homogenization

This chapter is comprised of a summary of the previous research in the relevant field. Techniques related to homogenization and de-homogenization are discussed.

Chapter 4: Method

In this chapter, the definition of homogenization, de-homogenization, equivalence theory, and generalized equivalence theory are discussed. Additionally, this chapter includes a brief introduction to the neutron transport code DRAGON and the neutron diffusion code DONJON. The code structures and data structures are discussed. There is a short discussion on the modules used in the input file.

Chapter 5: Models

This chapter includes the design of the DARGON model for lattice cell calculations and cross-section generation. Short description of the pin-by-pin power estimations is given. The design of the DONJON lattice cell model is presented.

Chapter 6: Results and Discussion

In this chapter, results tables comprised of calculations with general homogenization and de-homogenization are presented. Results are compared and discussed.

Chapter 7: Conclusion

This chapter has the summary of the work done during the research, and subsequently, conclusion of the work are stated.

CHAPTER 2: PROBLEM STATEMENT

2.1: Introduction

A pressurized water reactor (PWR) is a kind of LWR. In a PWR, the reactor core consists of slightly enriched uranium dioxide fuel rods that are cladded with Zircaloy. Zircalloy has low neutron absorption ability. It also consists of assorted interior constructions, reactivity controlling parts, and core monitoring apparatus. In the reactor core, pressurized light water acts as both coolant and moderator. The pressurized water is maintained under a saturation pressure. This leads to no significant volume of boiling in the reactor. It is one of the differences between PWRs and BWRs.

Table 2.1: Typical Reactor Core Parameters

	2-Loop Plant	3-Loop Plant	4-Loop Plant
Total heat output, MWt	1882	2785	3411
Heat generated in fuel, %	97.4	97.4	97.4
Nominal system pressure, psia (bar)	2250 (155)	2250 (155)	2250 (155)
Total coolant flow rate, lb/hr (kg/sec)	~71.03 x 10^6 (8950)	~109.0 x 10^6 (13734)	~138.4 x 10^6 (17438)
Coolant temperature			
Nominal inlet, °F (°C)	549.9 (287.7)	557.0 (291.7)	557.5 (291.9)
Average rise in vessel, °F (°C)	66.2 (36.8)	62.9 (34.9)	61.0 (33.9)
Outlet from vessel, °F (°C)	616.1 (324.5)	619.9 (326.6)	618.5 (325.8)
Equivalent core diameter, ft (cm)	8.4 (256)	9.98 (304)	11.06 (338)
Core length, between fuel ends, ft (cm)	12.0 (365.8)	12.0 (365.8)	12.0 (365.8)
Fuel type	16 x 16 Std	17x17 OFA	17x17 OFA
Fuel weight, uranium in core, kg	49,702	66,411	81,639
Number of fuel assemblies	121	157	193

[Westinghouse Electric Corp, 1984]

In a typical PWR reactor core, the fuel rods are structurally arranged in 17 x 17 square array in a fuel assembly. About 1/3rd of the total fuel assemblies are for the control rods. These fuel assemblies are tucked in by guide tubes. For the reactor control, other rods are filled by core machinery and burnable poisons such as boron. This extends the life of reactor core.

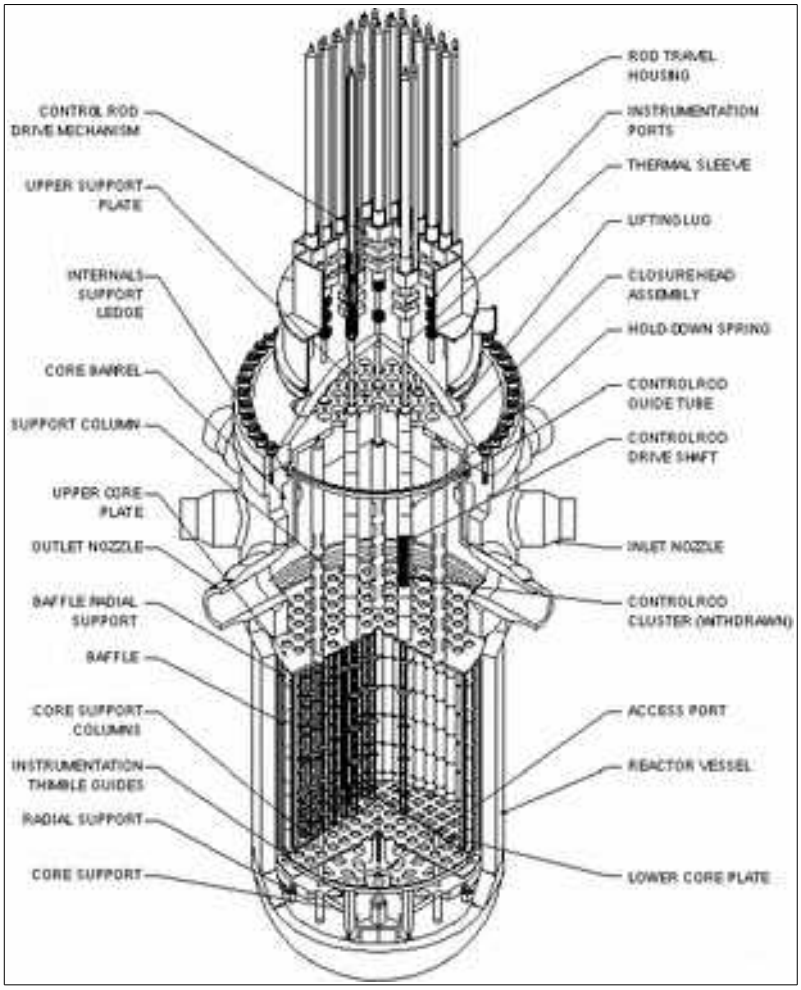

Figure 2.1(a) : PWR fuel assembly with control rod drive [wikipedia]

The fuel in the reactor core comprised of uranium dioxide (UO_2) pellets (enrichment of 2.1 - 3.1 %) in U^{235}. These pellets are 0.32 inches in diameter. The Length is 0.6 inches. The fuel rod length is about 12 feet and lattice pitch is about 0.496 inches.

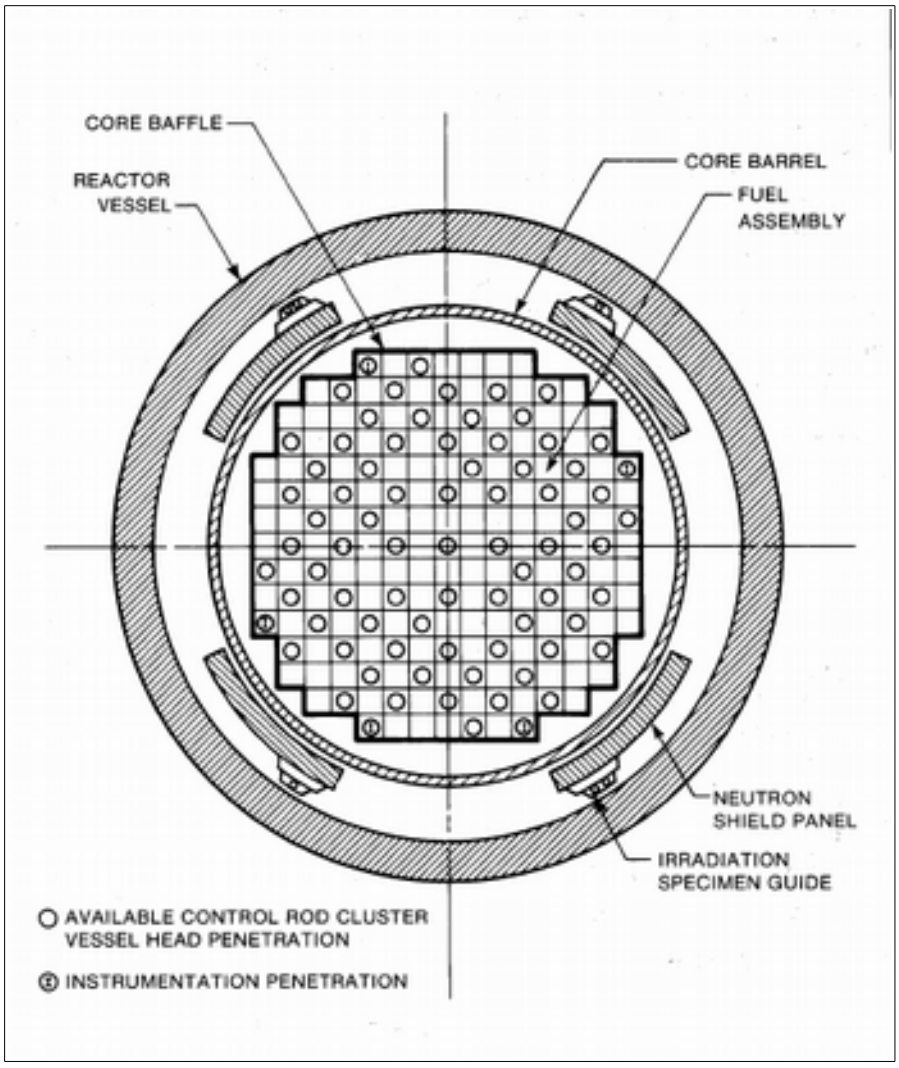

Figure 2.1(b): Cross-section of typical PWR core

[Westinghouse Electric Corp, 1984]

In a PWR, any accidental cladding breach is minimized by the lattice cell for following reasons. The first reason is to keep the fission

product. The second reason is to resist deterioration. This deterioration can be caused by high-temperature water [Westinghouse Electric Corp, 1984].

2.2: Standard Homogenization

Multigroup neutron transport equation (1.10) for the full core becomes complicated for the large reactor. Solving this equation with a large number of unknown variables is a challenging task. Thus, the problem is simplified by replacing detailed geometrical representation of the core with a simplified one. In this process, the cross-sections are averaged over each lattice cell. This averaging procedure is referred to as standard homogenization, and it is useful in reducing the size of the mathematical problem.

All facets of the heterogeneous estimations cannot be kept. It is not feasible either. The homogenized system is used for producing accurate overall approximated values which can depict the exact original system.

When homogenized properties are formed, these lattice cell-homogenized cross-sections are used with the two-group diffusion equations (1.14) and (1.15) are used for the full core calculations. The multi-dimensional and multigroup transport equation is first solved. The cell-homogenized and group-condensed cross-sections

are computed by using many energy groups (typically more than 50) with a detailed geometrical model for a lattice cell. The average cross-sections are then calculated. The flux-weighted averages over the lattice cell as shown in equations (2.1) and (2.2).

$$\overline{\phi_{RG}} = \frac{\sum_{r \in R} V_r \sum_{g \in G} \phi_{rg}}{V_R} \qquad (2.1)$$

$$\overline{\Sigma^{x}_{(RG)}} = \frac{\sum_{r \in R} \sum_{g \in G} \Sigma^{x}_{(rg)} \phi_{rg} V_r}{\overline{\phi_{RG}} V_R} \qquad (2.2)$$

$\overline{\phi_{RG}}$: average flux over a large region (in this case, one lattice cell) with volume V_R and a coarse energy group G

ϕ_{rg} : flux in a smaller region (calculated to capture neutron behaviors in small regions) with volume V_r and a fine energy group g

x : total or scattering or fission cross-sections

$\overline{\Sigma^{x}_{(RG)}}$: generic homogenized macroscopic cross-section for the large region V_R and coarse energy group G

$\Sigma^{x}_{(rg)}$: generic macroscopic cross-section in the small region V_r over the fine energy group g

Due to the heterogeneity present in the large region V_R , this procedure leads to the loss of information at assembly and pin levels.

Figure 2.2 shows a graphic depiction of the standard homogenization. The different color represents a different level of the irradiation e.g. freshly fueled channel, the channel with mid-burnup and discharge burnup bundles.

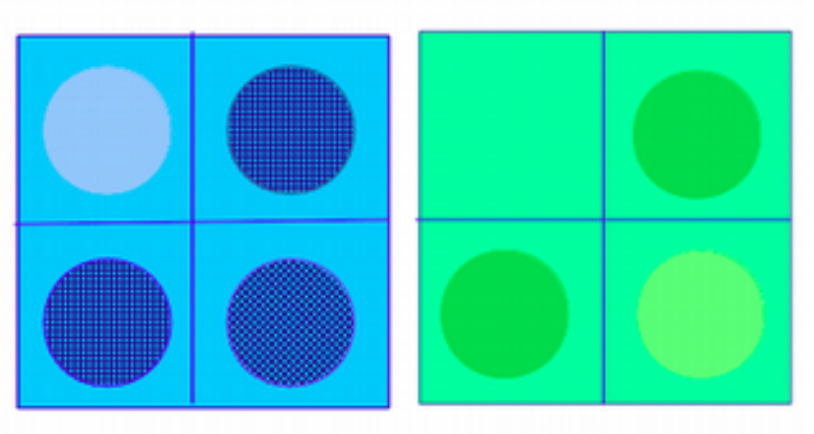

Figure 2.2: Pictorial representation of the standard homogenization method

2.3: Problems with Standard Homogenization

In standard homogenization, the transport equation is solved to produce the desired cross-section properties. For a single lattice cell, Reflective boundary conditions is also used to generate the homogenized properties. This is done by not considering the state of fuel bundles in the adjacent lattice cells. This procedure makes it susceptible to homogenization errors [Shen, 2006]. The homogenized cross-sections generated through equations (2.1) and (2.2) do not produce precise results for strong neutron absorbing materials [Robinson, 1995]. The errors are induced due to the heterogeneity

present in the lattice cells. Furthermore, the homogenized cross-sections produced through the standard homogenization technique could not maintain the reaction rates across the transport and diffusion models.

When a freshly fueled channel is present adjacent to a channel with high (discharge) burnup fuel, the standard homogenization cannot manage large reactivity changes in small spaces [Dall'Osso, 2006]. Additionally, when large regions of reflector material are present near the peripheral channels, it always plays a factor in inducing errors in produced cross-sections by standard homogenization method.

CHAPTER 3:

PROGRESS TO DATE IN PWR HOMOGENIZATION

Homogenization of a system means that heterogeneous elements of the system are superseded with homogeneous elements for a complicated and large system. This greatly reduces the computation time. Homogenized macroscopic cross-sections acquired using standard homogenization utilized with the diffusion induces inaccuracies in results nearby boundaries, neutron sources and neutron absorbers. This also reduces some variables of the original neutron transport equation.

Bettering the homogenization methods and reducing inaccuracies in results produced by diffusion theory have been an active area of research for more than the last 40 years. The Generalized Equivalence Theory (GET) addressed the issue of preservation of reaction rates in both Equivalence Theory and Generalized Equivalence Theory [Smith, 1980]. In GET, the integral flux is interrupted at the inter-lattice boundary to make the inter-lattice leakage accommodated. To achieve the discontinuity, integral flux is multiplied by “discontinuity factors”. When GET is applied to PWR fuel assembly with reflective boundary conditions, assembly Discontinuity Factors (ADF) are produced. When GET is applied to PWR fuel assembly with proper boundary conditions with leakage

representative of the target problem, exact discontinuity factors are produced.

The accuracy of diffusion calculations is improved by Aragones and Anhert (1986) by setting up an iterative process. In this process, they used a linear discontinuous finite difference diffusion formulation. Interface flux discontinuity factors are implemented to counter the erroneousness of standard homogenization. By applying limited incremental corrections to the diffusion coefficients, discrete finite difference expansion and spatial discretization are implemented to ensure the generation of diagonal dominance for the matrices. A rapid and stable convergence of the eigenvalues in PWR lattice cells surrounded by high reflector boundaries is achieved by this technique. However, this method required the incremental correction calculations. These correction calculations had to be executed individually in-between each local and global calculation steps.

In 1989, Rahnema produced a method to compute lattice cell cross-sections as a function of boundary conditions. It was done with the formulation of boundary condition perturbation theory for amelioration in capturing the environmental effects. These effects were caused by inter-lattice leakage that may emerge due to a high discrepancy in burnup between fuel bundles in adjacent channels.

Further improvements were done by Kim and Cho (1993). They applied a better iterative scheme for generation of lattice cell cross-sections. In this case, flux weighted constants and variational principles (Pomraning, 1967) were utilized for PWR and BWR. The boundary conditions for fuel assembly cross-section generation and the boundary conditions from both surface flux and leakage calculation were devised to be used in diffusion codes for the full core. Afterward, they achieved results with similar accuracy by using assembly discontinuity factors (ADF).

“Rehomogenization”, introduced by Smith (1994), was a different method that generated the homogenized cross-sections through recalculation in each step. He avoided the adjustment of discontinuity factors in each iteration in his method for lattice cell homogenization. However, this computational method was dependent on precise geometry definition of the inter-lattice regions. This method had no advantage of corrections which could have been accomplished by correcting the discontinuity factors in each step.

A method of corrections of the homogenized cross-section and discontinuity factors by applying the linear interpolation on homogenized parameters pre-calculated during the transport calculations was presented by Rahnema and Nichita (1997). The homogenized cross-sections and discontinuity factors built on the

actual boundary conditions at each lattice cell boundary was corrected by this method. In diffusion theory, this method was successfully applied for the Boiling Water Reactors (BWRs). The approximations used in this method could not manage strong heterogeneity.

Clarno and Adams et al. (2003) computed for environment effect on leakage in the presence of multiple fuel assemblies. These fuel assemblies contained MOX and UO_2 fuel. The models used were 1D and 2D models with various configurations. They obtained promising outcomes for fuel assemblies for certain configurations.

Herrero et al. (2012) presented a function fitting method. This method utilized the environmental effects on the computed cross-sections instead of producing discontinuity factors. This method used a simplified Analytic Coarse Mesh Finite Difference (ACMFD) function. The interacting energy group terms were counteracted and eliminated by ACMFD in the cell buckling calculations. This method produced a good set of cross-sections for pin-by-pin diffusion calculation.

Gomes (2012) used finite element codes to determine the efficaciousness of the Assembly Discontinuity Factor (ADF) for highly heterogeneous fuel assemblies with multiple fuel types and different

burnups. He deduced that it is essential to utilize ADF to improve results for highly heterogeneous configurations in PWR.

Dall'Osso (2006) came up a modified rehomogenization technique. In which, he introduced a delta cross-sections coefficient. To account for environmental effects, delta cross-section coefficients were generated with the standard homogenized cross-sections. These methods showed amelioration in keeping reaction rates across the models. It also showed an improved estimation of control rod worth.

Merk and Rohde et. al. (2011) presented a technique that applied reflective boundary condition inside the PWR fuel assembly for transport calculation which improved efficiency in calculations. The two group diffusion equation with an external source on a homogenous 2D model was empirically solved. It eliminated the extra iterations compared to the methods using discontinuity factors.

The application of Superhomogenization was one of the most substantial steps in improving homogenization methods to maintain the reaction rates across the transport and diffusion models. Hebert et al. (1993) showed the use of superhomogenization factors. Superhomogenization accommodates homogenized cross-sections by multiplying superhomogenization (SPH) factors. This process accomplishes equality between the reaction rates in the

homogeneous model and in the heterogeneous model. The problems with different diffusion models could be addressed by these factors. It removed the need of multiple iterations or modification of the diffusion code. Overall, SPH factors produced propitious results in control rod worth measurements for pin-by-pin homogenization. However, SPH factors are used with sub-cell homogenization and required extra spatial discretization. This leads to extra computation and time. Though, additional computation might not be a problem in the future with the growth of technology.

Robinson and Tran (1995) developed a reaction rate conservation technique. This technique is similar to SPH method. They obtained some improved outcomes compared to standard homogenization technique.

In 2013, Berman et. al pointed out inadequacies in the application of SPH when surface currents are preserved. He recommended that the surface currents could be preserved by using adjusted diffusion coefficients. It is assumed that the boundaries are all reflective in the process of SPH factor generation. However, during the generation of SPH factors, the overall buckling is accommodated. Thus, the eigenvalue is reduced to one. It is supposed to account for nonzero surface currents.

Generalized pin-power reconstruction (GPPR) improved the inaccuracies in lattice cell homogenization by addition of small computational time [Fliscounakis, 2011]. Brosselard et al. (2014) improved this methodology. Using pin power reconstruction method, more details could be achieved at pin and assembly levels. This method is also called de-homogenization method for reactor core calculations. Hebert et. al. (2015) discussed some encouraging results for the pin power reconstruction methodology for PWRs using DRAGON5 and DONJON5.

There had been a lot of work done that showed some improvements in LWR computation accuracy. This improvement comes at the cost of additional computational steps and time. To reduce those extra computational expenses, there are some exceptional techniques. De-homogenization method looks promising because of its ability to circumvent those additional steps of calculations and preserve the details at assembly and pin levels that are otherwise lost in standard homogenization and superhomogenization methods.

CHAPTER 4: METHOD

To reduce the inaccuracies in lattice cell homogenization in PWR, the lattice cell is sub-divided into sub-cells and perform a sub-cell level homogenization. The goal of this study is the inspection of the 3 by 3 sub-cell homogenization for a typical PWR lattice cell using the de-homogenization technique for both heterogeneous and homogeneous geometries using SHEM 361 cross-section library.

4.1: Theoretical Background

A neutronic deterministic calculation is generally performed in two steps: assembly calculation, and full-core calculation. For performing the full reactor calculation, the multi-parameter database of homogenized cross-sections and other parameters is produced as the last step of assembly level calculation.

Superseding the heterogeneous elements with homogeneous elements is called homogenization. This simplifies of the large and complicated systems. Homogenization helps in reducing computation time and simplifies the transport equation by eliminating some variables.

The purpose of homogenization is to acquire precise averaged values that can represent the exact original system. A heterogeneous

calculation is not possible due to the high complexity of the reactor systems and computation time. However, homogenization process leads to loss of details at pin and assembly levels.

4.1.1: Equivalence Theory

For homogenization process, the first step is choosing reactor properties. These properties are later homogenized. Considering these properties of interest,

$$\int_{V_i} \tilde{\Sigma}_g(\boldsymbol{r})\tilde{\phi}_g(\boldsymbol{r})\,d\boldsymbol{r} = \int_{V_i} \bar{\Sigma}_g(\boldsymbol{r})\bar{\phi}_g(\boldsymbol{r})\,d\boldsymbol{r} \qquad (4.1)$$

$$\int_{S^k_{(i)}} \nabla . \tilde{\boldsymbol{J}}_{\boldsymbol{g}}(\boldsymbol{r})\,d\boldsymbol{S} = \int_{S^k_{(i)}} \nabla . \bar{\boldsymbol{J}}_{\boldsymbol{g}}(\boldsymbol{r})\,d\boldsymbol{S} \qquad (4.2)$$

$$\tilde{k}_{eff} = \bar{k}_{eff} \qquad (4.3)$$

Here,

$\tilde{\phi}_g(\boldsymbol{r})$: integrated flux for correspondent homogeneous problem

$\bar{\phi}_g(\boldsymbol{r})$: integrated flux for exact heterogeneous problem

$\tilde{\boldsymbol{J}}_{\boldsymbol{g}}(\boldsymbol{r})$: integrated current correspondent homogeneous problem

$\bar{\boldsymbol{J}}_{\boldsymbol{g}}(\boldsymbol{r})$: integrated current exact heterogeneous problem

$\tilde{\Sigma}_g(\boldsymbol{r})$: total cross-section correspondent homogeneous problem

$\bar{\Sigma}_g(\boldsymbol{r})$: total cross-section exact heterogeneous problem

$\tilde{k}_{eff}$: multiplication factor correspondent homogeneous problem

$\bar{k}_{eff}$: multiplication factor exact heterogeneous problem

An ideal homogenized cross-section can be determined if it is assumed that homogenized parameters are spatially constant for region i of volume V_i .

$$\widetilde{\Sigma}_g^i = \frac{\int_{V_i} \bar{\Sigma}_g(\boldsymbol{r})\bar{\phi}_g(\boldsymbol{r})\,d\boldsymbol{r}}{\int_{V_i} \widetilde{\phi}_g(\boldsymbol{r})\,d\boldsymbol{r}} \tag{4.4}$$

For the simplification of the homogenized system, integrated surface current is preserved by depending on a low order operator. So, according to Fick's law, the correlation of the neutron current and the gradient flux is given as:

$$\widetilde{D}_g^i = \frac{-\int_{S_k^i} \bar{\boldsymbol{J}}_{\boldsymbol{g}}(\boldsymbol{r})\,d\boldsymbol{S}}{\int_{S_k^i} \nabla \widetilde{\phi}_g(\boldsymbol{r})\,d\boldsymbol{S}} \tag{4.5}$$

First, satisfying solutions of both heterogeneous and homogeneous systems must be found for Equations (4.4) and (4.5). Second, nonlinearity is observed to be introduced in above equations. Third, the homogenized diffusion coefficient in Equation (4.5) must be defined. Each node is characterized by the k surface. The issue presents itself when the same amount of diffusion coefficients need to be defined each node is characterized by the k surface as the number of nodes characterized by the k surface. Determination of a spatially variable that is both constant and unique is not attainable.

Thus, keeping both average reaction rate and surface approximated group current is also not possible.

However, several methods are available to address the above issues. The most common method is to the homogenization of heterogeneous system. In this method, it is surmised that an infinite lattice estimation is enacted by enforcing reflective boundary conditions. By working out a two-dimensional heterogeneous neutron transport equation on a finite part of the precise system, the precise homogeneous outcome is obtained.

However, the inaccuracies appear in this method for the large and complicated systems. In case of large and complex systems, macro-regional flux gradients are spatially produced at the different nodal junction. The issue of preservation of surface integrate currents cannot be resolved by the use of the spatially-constant diffusion constants. The continuity of flux at the nodal junction is kept a limit for the diffusion calculation. It is done for the preservation of reaction rates and surface integrate current

4.1.2: Generalized Equivalence Theory

The Generalized Equivalence Theory (GET) confronts the issue of preservation of reaction rates in both Equivalence Theory and Generalized Equivalence Theory by adding degrees of freedom. In

GET, the integral flux is interrupted at the inter-lattice boundary to make the inter-lattice leakage accommodated. To achieve the discontinuity, integral flux is multiplied by “discontinuity factors”.

When GET is applied to PWR fuel assembly with reflective boundary conditions, assembly Discontinuity Factors (ADF) are produced. When GET is applied to PWR fuel assembly with proper boundary conditions with leakage representative of the target problem, exact discontinuity factors are produced.

Assuring the continuity of the homogeneous flux at the nodal junctions, the interface condition for each energy group:

$$f^{\wedge}_{(g,j)} \int_{S_j} \hat{\tilde{\phi}}_g(\boldsymbol{r})\, d\boldsymbol{S} = f^{\vee}_{(g,j)} \int_{S_j} \check{\tilde{\phi}}_g(\boldsymbol{r})\, d\boldsymbol{S} \qquad (4.6)$$

Where,

$f^{\wedge}_{(g,j)}$: energy depending on discontinuity factors at the surface S_j and the surface approximated homogeneous flux $\hat{\tilde{\phi}}_g$

$f^{\vee}_{(g,j)}$: energy depending on discontinuity factors at the surface S_j and the surface approximated homogeneous flux $\check{\tilde{\phi}}_g$

If the heterogeneous flux is continued at the interface, both reaction rates and surface net currents are preserved.

On an individual assembly with reflective boundary conditions, the heterogeneous problem is analyzed with the large-scaled approximated cross-sections and diffusion coefficients turning almost equal to the flux-volume weighted parameters. It is surmised that the homogeneous flux is flat in the homogenized node. This turns the intermediary heterogeneous flux and the approximated homogeneous flux same computationally by definition. Then,

$$adf_{(g,j)} = \frac{\tilde{\phi}_{(g,j)}}{\bar{\phi}_{(g,j)}} \qquad (4.7)$$

$adf_{(g,j)}$ is the assembly discontinuity factor (ADF). This method minimizes the computational time and decreases the number of calculation steps of equivalence parameters for each type of assembly.

4.1.3 Dehomogenization

Performing reactor core calculations with homogenized cross-sections leads to loss in details. This level of details can be retained by pin-power-reconstruction (PPR) method as precisely as possible. This process is also called de-homogenization technique for nuclear reactor core calculations. Though, additional computing time is required as compared to classical methods.

For arbitrarily homogenized geometries, generalized pin power reconstruction method was first proposed by Fliscounakis et al. (2011). The basic idea behind the de-homogenization technique is to see the detailed flux distribution ϕ_D as the multiplication of the macro-flux ϕ_m and the local flux ϕ_l . ϕ_m is provided by the large-scaled estimation and denotes the conventional shape of flux at reactor core level. At the assembly level, ϕ_l denotes the ripple-shaped flux and it is produced from the neutron transport calculations.

The reaction rate for each pin is given by:

$$\tau_{(i,p)}^{Gen} = \tilde{\Sigma}_{(p,ref)} x\, \phi_{(i,p)}\left(\tilde{\Sigma}_i\right) x \frac{\phi_p^{\infty}\left(\Sigma_p\right)}{\phi_{(1,p)}^{\infty}\left(\Sigma_i\right)} \cdot V_p \qquad (4.8)$$

$$with\ 1 \le i \le M \wedge 1 \le p \le P$$

$$\tau_{(i,p)}^{Gen} = \tilde{\Sigma}_{(p,ref)} x\, \tilde{\phi}_{(i,p)}\left(\tilde{\Sigma}_i\right) x \frac{\phi_{(p,ref)}}{\lambda_p \phi_{(1,p)}^{\infty}\left(\Sigma_i\right)} \cdot V_p \qquad (4.9)$$

In equations (4.8) and (4.9), i & p denotes the projection of the large scaled estimated flux on the pin-by-pin geometry. Equation (4.9) was proposed by Brosselard et al. (2014). In equations (4.8) and (4.9), the actual flux may not be same as the reference flux. It is only the large-scaled estimated flux projection on each pin. The shape factor fixes this error and denotes the proportionality between the large scaled estimated fluxes enacted over a pin-by-pin geometry. The same is also estimated for the heterogeneous geometry. When

general geometry is used instead of pin-by-pin geometry, the shape factor denotes the relative error.

Through the de-homogenization method, the actual heterogenous structure inside each node could be reconstructed after the nodal calculations are done. The nodal flux solutions are combined with form functions to assure a thorough regeneration of the heterogeneous power in an individual node. GFF (Group Form Function) is estimated from the lattice computations. This Groupwise factor considers the identical averaging of ADF in regards to the infinite lattice approximation.

$$f_g(x,y)=\frac{K\Sigma^{\sim}_{(f,g)}\varphi_g(x,y)}{K\Sigma^{\sim}_{(f,g)}\varphi^{-}_{(f,g)}} \qquad (4.10)$$

Where,

$K\Sigma^{\sim}_{(f,g)}$: large scaled fission cross-section of the fuel in group g manifolded by the energy originated from fission.

Corner discontinuity factor (CDF) is required to be defined due to the dehomogenization technique. This is done in the interest of keep trails of the regional heterogeneities that are present at the junction between assemblies.

In case of CDFs, the flux is retrieved at the corner of the assembly:

$$CDF_{(f,g)} = \frac{\tilde{\phi}_{(g,j,corner)}}{\bar{\phi}_{(g,j)}} \tag{4.11}$$

4.2: Computational Tools

For this research, the neutron transport code DRAGON [Marleau, 2009], and the neutron diffusion code DONJON [Varin, 2005] are used for computing. These open source codes are built at École Polytechnique de Montreal and widely used to perform lattice cell and full-core calculations. These codes are intended to be “Industrial Standard Toolset” (IST) components for the Canadian nuclear industry.

DRAGON Version 5 was introduced in 2014 and modified later up to 2017. This version is a 64-bit clean delivery. In this version, acceleration of step and linear discontinuous schemes are applied for MOC. Other changes include integration with external CAD tool like SALOME, G2S: module for windmill-type geometry discretization that do not need external CAD tool.

These computational codes have datatype as linked lists. These functions are modules. Input scripts are written in CLE-2000 language. The input deck is essential for linking the required cross-section data file and create an “access” file. When *.access script is

not provided, tdraglib.access file is automatically used by DRAGON. A brief description of the codes is provided in this chapter.

4.2.1: DRAGON5

DRAGON is a lattice code used to solve the neutron transport equation by enforcing multifarious numerical and estimation methods. The code performs the neutron transport calculations by using multidimensional geometry using the collision probability (PIJ) method and MOC including interface current (IC) [Hebert, 2015].

The lattice cell code divided into several calculation modules which can be called by GAN generalized driver and provides a template to build applications by linking independent modules. Each module in the code is linked and data is exchanged between the modules via linked lists to perform an elementary task [Marleau, 2015].

Method of characteristics (MOC) is founded on the repetitive estimation of particle flux by solving the multi-group transport equation above the trails passing through the zone. The characteristic model of the transport equation is solved using the trailing of the straight neutron paths as the neutron moves across the zone [Askew, 1972].

For this study, MOC is used for solving the transport equation. A PWR-lattice-cell geometry was modeled.

4.2.2: DONJON5

DONJON is a code (part of DRAGON package) that is designed to execute full reactor core diffusion calculations. The DONJON Version5 is reprogrammed around the GANLIB5 kernel [Herbert, 2015]. It has its roots in TRIVAC-3, GANLIB, UTILIB, DRAGON codes.

The deterministic approach for solving 2D and 3D multi-group diffusion equation is followed by DONJON code. DONJON code divided into several calculation modules which can be called by GAN generalized driver and provides a template to build applications by linking independent modules. For DONJON requirements, reactor material properties are obtained from DRAGON.

For this study, geometries represent homogenized volumes of PWR fuel bundles which are modified for group form function (GFF) and heterogeneous database. The environmental effects are not considered. The lattice estimations are done with the infinite lattice approximation.

4.2.3: DRAGON and DONJON Code-Input Structure

The DONJON and DRAGON require three major elements in input script. These key elements are definitions of reactor materials. definition of geometry, and definition of solution control. Below, a typical schematic of the DRAGON/DONJON input structure [Marleau,2009] is given.

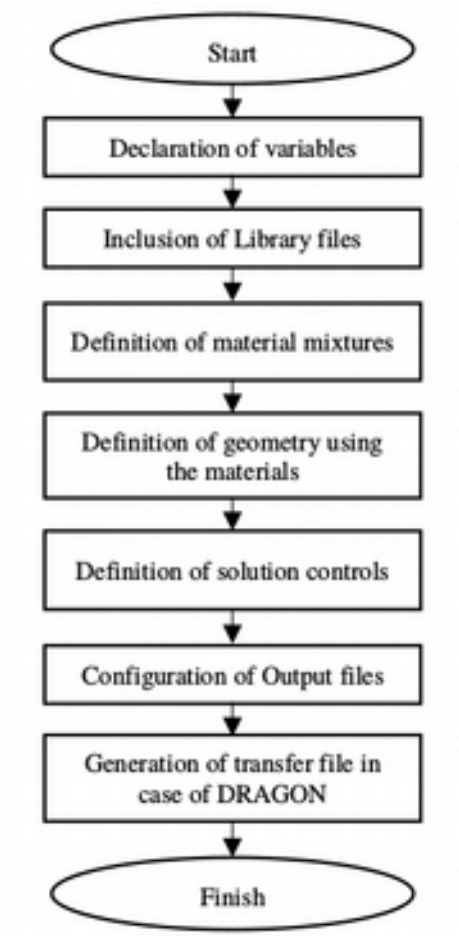

Figure: 4.1: Schematic of the input file structure for DRAGON/DONJON [Marleau,2009]

The declarations of variables and reference to microscopic cross-sections library files are essential for key elements above. The output file can be designed as per the user's needs.

4.2.4: Modules

The DRAGON and DONJON code's input decks usually follow a specific order of modules. For example, geometry module must be defined before tracking module or flux module. This is done because the resulting files of a module most often are used as input in the following modules.

Various modules are present in both codes to execute different functions analogous to solving the transport or diffusion equations. Below, some modules that are mentioned in the DRAGON code are explained [Marleau, 2014].

LIB: Used for generating or modifying a DRAGON microlib.

GEO: Used for definition or modification of geometry.

SYBILT: Used for standard tracking on the basis of 1D collision probability or Interface Current technique

EXCELT: This is the standard full cell collision probability tracking module for 2D and 3D geometries. It is also used for isolated 2D cells containing clusters.

MCCGT: This module is based on MCCG code (Method of Characteristics in Complex Geometry) and used for tracking.

BIVACT: This module is used for tracking 1D/2D diffusion and SP_n. It is a BIVAC-type tracking along with finite element discretization.

UTL: Used for manipulating a data structure.

GREP: Used for tracking information on a data structure.

EVO: This module is used for burnup calculations.

COMPO: This module generates the multi-parameter reactor database.

Some modules that employed by DONJON are explained below. [Hebert, 2014]

GEO: This module is used for MIX record.

USPLIT: This module is used to generate an extended reactor material index over the complete mesh-splitted reactor geometry.

TRIVAA: This module is used to compute the set of system matrices with respect to the previously obtained ”tracking” information

RESINI: This module used to define the fuel lattice. This generates the fuel-map geometry and specifies the global and local parameters.

TRIVAT: This module is used to carry out a 3-D numerical discretization.

MACINI: This module is used for generating an extended macrolib. The properties are saved per each material domain over the whole mesh-splitted reactor geometry.

NCR: This module is used for creating a microlib or a macrolib containing the material properties.

FLUD: This module is used to numerically computing the diffusion equation for the flux and eigenvalues.

NAP: This module is used for pin power reconstruction.

4.3: Calculation Steps

The following methodology is used for the investigation of the 3 x 3 sub-cell homogenization for a typical PWR lattice cell. Firstly, for a PWR lattice cell, a heterogeneous geometry MULTICOMPO database file is generated using transport code DRAGON at zero burnup.

This multicompo database file is used in the diffusion model for the lattice cell generated using the diffusion code DONJON. The diffusion and transport equations are different as previously discussed in sections 1.1 and 1.2. Thus, the solution of the eigenvalues and fluxes are also different for both codes.

Using DONJON 5, diffusion flux on a homogenize assembly in an infinite space is computed and the output file is in COMPO format. This database is further used to perform pin power reconstruction

for both homogeneous homogenization and heterogeneous homogenization. The pin by pin geometry is also used to visualize the heterogeneous homogenization.

CHAPTER 5: MODELS

This chapter represents different calculation schemes and model used for DRAGON5 and DONJON5 calculations. With reflective boundary conditions, a 3 x 3 PWR assembly layout is taken into account. This structure can be modified for various fuel configurations with an intermediary fuel assembly of UOX or MOX or UOX as shown in Figure 5.1.

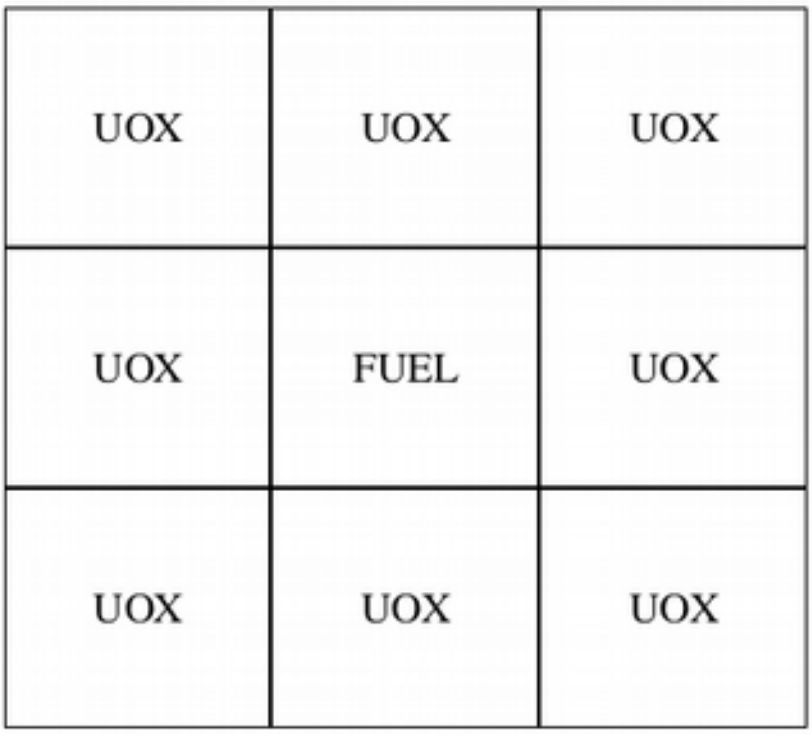

Figure 5.1: 3 X 3 PWR assembly configuration

In the diffusion calculation, nine assembly nodes are considered with the dimension comparable to a lattice pitch. It is important to note that the assembly model is chosen in such a way that this model cannot be used to obtain a core critical configuration and doesn’t

contain quasi-critical cluster. Leakage model of the lattice calculation has an important effect in the evaluation of the outcomes.

5.1: Lattice Schemes

For Light Water Reactors assemblies, new advances in DRAGON5 [Hébert, 2014] let the added degree of freedom in designing numerical schemes for deterministic computations.

Recent improvements in DRAGON5 package includes the integration with external tools like SALOME [Hébert, 2014], the applicability of the Subgroup Projection Method (SPM) with bettered 295 or 361 group libraries known as SHEM 295 and SHEM 361 [Hébert (2009)], two-level computational scheme [Canbakan, 2015] and De-homogenization method or Pin Power Reconstruction [Chambon, 2015].

For the subgroup projection method in this study, SHEM 361 group energy mesh library is used in the computations. Santamarina-Hfaiedh energy mesh (SHEM) refined the energy group between 22.5 eV and 11.14 keV, and therefore, optimizing 281-group to accommodate the SPM [Hfaiedh, 2006]. Cross-sections are used in DRAGLIB format.

In the two-level scheme, the methodology is divided into two steps:

1. A first-level double P_1 interface current calculation is performed over the refined energy 361-energy group mesh to get fast flux. In this step, Superhomogénéisation (SPH) can be calculated [Hébert, 2009]. This should be done before the second step. In this study, SPH calculations are not done. This study is done at zero burnup.

2. In this step, a thorough another level flux measurement enforced using the method of characteristics (MOC) on the group labyrinth. It was quantized over a refined spatial labyrinth.

As a last step of the calculation, the homogenized cross-sections and flux distribution are wielded to breakdown cross-sections into two categories of groups with the threshold at 0.625 eV (fast group for above 0.625 eV & thermal group for below 0.625 eV) and the resulted data are saved in the multi-parameter database.

Below, the schematic diagram of the 2-level computational scheme for DRAGON5 lattice code [Canbakan, 2015] is given.

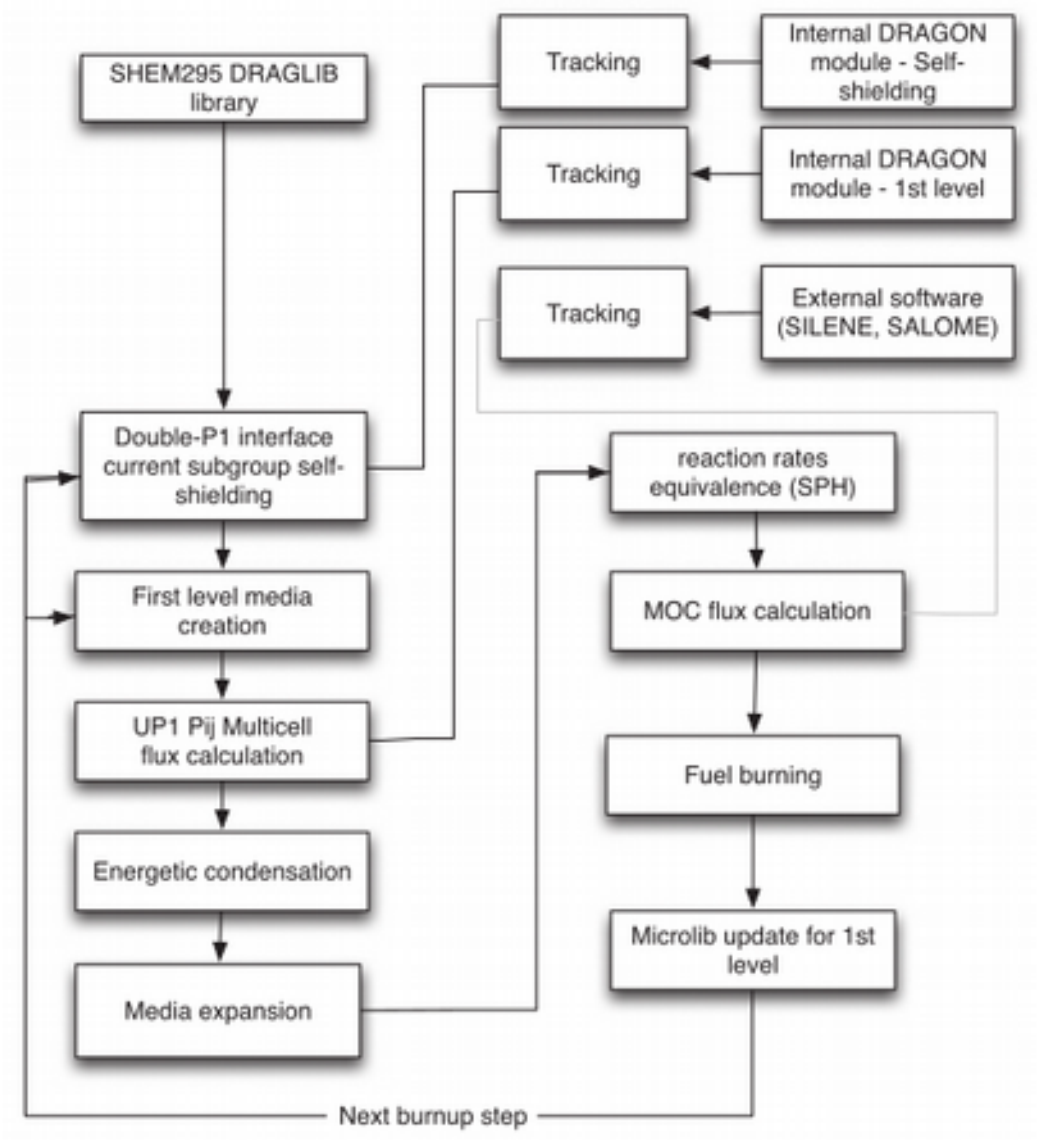

Figure 5.2: 2-level computational scheme for DRAGON5 lattice code [Canbakan, 2015]

In this work, diffusion, transport, and PPR computations are optimized for DRAGON5 with SHEM361 library using the two-level computational scheme and pin power at each assembly level for a 3 x 3 assembly configuration is calculated. Comparision is done for

between homogeneous homogenization and heterogeneous homogenization[Chambon, 2015].

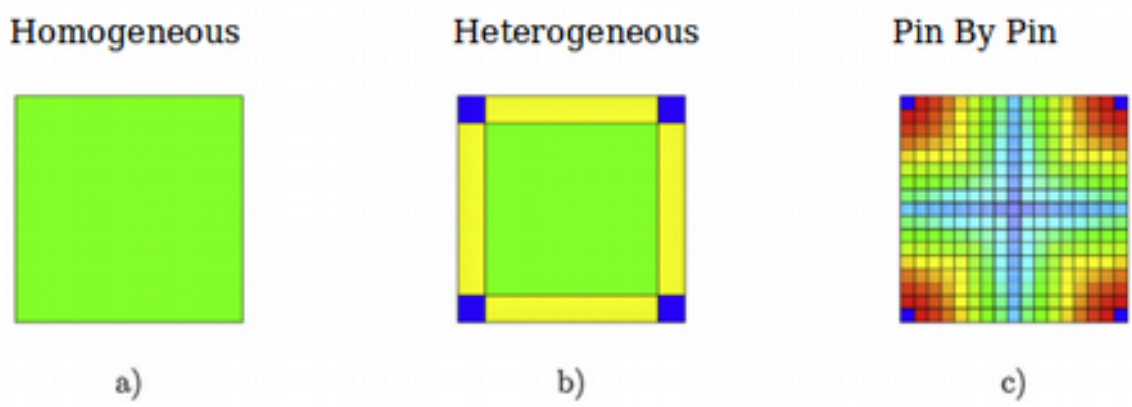

Figure 5.3: Homogenization geometries [Chambon, 2015]

Three types of homogenization are demonstrated in figure 5.3. The heterogeneous homogenization is composed of three combinations i.e. center of the assembly, side of the assembly, and corner of the assembly. Two series of pins are used to define the side. In this study, we are performing heterogeneous homogenization and homogeneous homogenization.

5.2: Cross-Section Preparation

From the lattice calculation done by DRAGON5 code, macroscopic cross-section data is produced and stored in a multi-parameter database. This multi-parameter database obtained from DRAGON5 code is further used to compute diffusion flux on a homogenize assembly in DONJON5 code once for heterogeneous homogenization

and once for homogeneous homogenization. To perform the PPR or de-homogenization, the multi-parameter database file is generated for homogeneous option and heterogeneous option for calculations using different properties (homogeneous, heterogeneous and pin by pin properties).

CHAPTER 6: RESULTS AND DISCUSSION

To validate the Pin Power Reconstruction or Dehomogenization, three homogenization types can be enacted as depicted in Figure 5.3. The heterogeneous homogenization is composed of three combinations i.e. center of the assembly, side of the assembly, and corner of the assembly. Two series of pins are used to define the side. In this study, we are performing heterogeneous homogenization and homogeneous homogenization.

6.1: Results Using DRAGON5

For 3 x 3 PWR colorset assembly configuration, the calculations are done using DRAGON 5 code for the generation of heterogeneous and GFF MULTICOMPO data structure output. These calculations are done at zero burnup and self-shielding using subgroup projection method. In this study, UOX denotes UO_2 fuelled and MOX denotes multi-zone $UpuO_2$ fuelled. For the subgroup projection method in this study, SHEM 361 group energy mesh library is used in the computations and therefore, optimizing 361-group to accommodate the SPM [Hfaiedh, 2006]. At zero burnup, normalized flux and k_{eff} are computed at zero burnup.

In this step, a MULTICOMPO database file is generated for heterogeneous geometry and GFF at zero burnup.

Table 6.1: DRAGON Results for UOX

Fuel Type	UOX
Isotope Volume	1.27008009E+01
Isotope Depletion	3.96024156E-03
k_{eff}	1.004327e+00
Normalized Flux	3.66138E+02

Table 6.2: DRAGON Results for MOX

Fuel Type	MOX
Isotope Volume	6.35039997E+00
Isotope Depletion	1.873753e-03
k_{eff}	1.001643e+00
Normalized Flux	4.10522E+02

6.2: Results using DONJON5

Diffusion power on a homogenized assembly in an infinite space is computed using DONJON5. Calculations are done first for homogeneous homogenization and for the heterogeneous homogenization.

The MULTICOMPO reactor database is assessed for two configurations of the colorset 3x3: with UOX assembly and with MOX assembly at the center of the layout as shown in Figure 5.1. In this study, ADF corresponding to the diffusion calculation equal to unity and B1 homogeneous model as leakage approximation is used for the lattice calculation.

The results with homogeneous heterogenization and homogeneous homogenization are presented in Tables 6.3, 6.4, 6.5 and 6.6.

Table 6.3:

Results using DONJON5 for homogeneous homogenization (UOX)

Fuel Type	UOX
k_{eff}	1.263637e+00
Transport Power	2684.49390
Diffusion Power (before normalization)	7.33851957
Diffusion Power (After normalization)	2684.50513

Table 6.4:

Results using DONJON5 for heterogeneous homogenization (UOX)

Fuel Type	UOX
k_{eff}	1.263712e+00
Transport Power	2684.49390
Diffusion Power (before normalization)	7.32114506
Diffusion Power (After normalization)	2684.49634

Table 6.5:

Results using DONJON5 for homogeneous homogenization (MOX)

Fuel Type	MOX
k_{eff}	1.115161e+00
Transport Power	1417.65662
Diffusion Power (before normalization)	3.45463300
Diffusion Power (After normalization)	1417.65588

Table 6.6:

Results using DONJON5 for heterogeneous homogenization (MOX)

Fuel Type	MOX
k_{eff}	1.115142e+00
Transport Power	1417.65662
Diffusion Power (before normalization)	3.46421456
Diffusion Power (After normalization)	1417.65747

6.3: Pin Power Reconstruction

During the implementation of PPR [Chambon, 2015], the first major problem comes with the flux projection on each pin. Using the **NAP:** module, pin by pin geometry is constructed. The outcomes are not accurate when the intermediate flux of each large scaled region is operated for the pin projection. When no large shaped regions are

considered locally, the flux is alike on assorted pins per assembly. To settle this issue, the polynomial depiction of the flux within a large scaled region is taken. Before the flux is distributed on the pin, estimation is done with the same polynomial order. Then, the large-shape of the flux can be considered the pin level. The next issue of the inaccuracy is produced during the regularity of the tracing between the core and infinite region computations.

Two homogenization geometries are tested. Instead of using the intermediate flux per assembly in case of heterogeneous homogenization, the intermediary flux on the neighboring series of the pin in Figure 5.3 is used [Liponi, 2017]. The results obtained from the computations are presented in Tables 6.6 and 6.7. The results are compared for power, flux, and k factor in Table 6.8.

Table 6.7:

Pin By Pin power and flux calculations for homogeneous homogenization

k_{eff}: 1.078156e+00		
Total Flux: 3.70291758		
Total Power: 5.59677044E-12		
Assembly	Power	Flux
1	0.766600907	1.97548866E-02
2	1.09802783	9.05148834E-02
3	0.766600788	0.177794009
4	1.09802735	0.362059444

5	1.54150677	0.627761722
6	1.09802842	0.814634264
7	0.766600609	0.967989504
8	1.09802699	1.44823873
9	0.766600966	1.60014439

Table 6.8:

Pin By Pin power and flux calculations for heterogeneous homogenization

k_{eff}: 1.078179e+00		
Flux: 3.66504478		
Total Power: 5.60789436E-12		
Assembly	Power	Flux
1	0.767510712	1.96884498E-02
2	1.09780347	9.00333747E-02
3	0.767511010	0.177196145
4	1.09780276	0.360133320
5	1.53877449	0.625273407
6	1.09780359	0.810300469
7	0.767510355	0.964734375
8	1.09780288	1.44053435
9	0.767510831	1.59476233

6.4: Comparisons

The k-eff, fluxes, power is calculated by using the de-homogenization technique in section 6.3. The errors in the k_{eff}, power, and flux ϕ are calculated based on the following equations.

$$\nabla k_{eff} = k_{eff}^{homogeneous} - k_{eff}^{heterogeneous}$$

$$\nabla Power = Power_{homogeneous} - Power_{heterogeneous}$$

$$\nabla Flux = Flux_{homogeneous} - Flux_{heterogeneous}$$

Errors are calculated between homogeneous homogenization and heterogeneous homogenizations:

Table 6.9: Error calculated between homogeneous homogenization and heterogeneous homogenization

Fuel Type	UOX	
Δ k_{eff}	- 0.000023	
Δ Flux	0.0378728	
Δ Total Power	1.11239E-14	
Assembly Number	Δ Power	Δ Flux
1	- 0.000909805	6.64368E-05
2	0.00022436	0.000481509
3	- 0.000910222	0.000597864
4	0.00022459	0.001926124
5	0.00273228	0.002488315
6	0.00022483	0.004333795
7	- 0.000909746	0.003255129
8	0.00022411	0.00770438
9	- 0.000909865	0.00538206

In the comparison in Table 6.9, the discrepancies between results obtained from both homogeneous geometry and heterogeneous geometry are negligible. However, the more accurate results are obtained with the heterogeneous geometry because it minimizes the error.

CHAPTER 7: CONCLUSION

In this study, the reconstructed pin power has been successfully optimized and computed with subgroup projection method for SHEM361 energy group using the 2-level scheme approach with MOC. For geometries, homogeneous geometry and heterogeneous geometry for a 3 x 3 PWR cluster are used. Using the NAP: module, a two levels computational scheme for the core with heterogeneous assemblies are generated. Enrich multi-parameter data structure was obtained to keep the projected flux per pin for diffusion calculations. It was done for homogenized assembly in an infinite region for different homogenization options.

It is observed that a great amount of time is saved when a thorough MOC calculation is conducted on a SHEM361 energy group mesh. Also, the 2-level computational method is showing optimistic results for deterministic computation. The generation of multi-parameters reactor databases also saves time in subsequent computations. Using the PPR, flux projections and power are calculated for both homogeneous geometry and heterogeneous geometry at each assembly pin. The results for both geometries are compared and discrepancies are calculated. It shows that heterogeneous geometry shows more accurate and promising results.

REFERENCES

1. Aragonés, J. M., & Ahnert, C. "A linear discontinuous finite difference formulation for synthetic coarse-mesh few-group diffusion calculations." Nuclear Science and Engineering 94.4 (1986): 309-322.

2. Berman, Y. "An improved homogenization technique for pin-by-pin diffusion calculations." Annals of Nuclear Energy 53 (2013): 238-243.

3. Brosselard, C., Leroyer, H., Fliscounakis, M., Girardi, E., Couyras, D., 2014. Normalization Methods for diffusion calculations with various assembly homogenizations. In: PHYSOR 2014, September 28–October 3, Kyoto, Japan.

4. Clarno, K. T., & Adams, M. L. "Capturing the effects of unlike neighbors in single-assembly calculations." Nuclear science and engineering149.2 (2005): 182-196.

5. Canbakan, A.& Hebert, A., “Accuracy of a 2-level scheme based on a subgroup method for pressurized water reactor fuel assembly models,” Annals of Nuclear Energy, 81, 164–173 (2015).

6. Chambon, R., “Implementation of pin power reconstruction capabilities in the DRAGON5/PARCS system,” Tech. Rep. IGE-349, École Polytechnique de Montréal (Canada (2015).

7. Dall’Osso, A. "A spatial rehomogenization method in nodal calculations." Annals of Nuclear Energy 33.10 (2006): 869-877.

8. Donnelly, J. V., Min, B. J., Carruthers, E. V., and Tsang, K. "Modeling of CANDU reactivity devices with WIMS-

AECL/MULTICELL and superhomogenization." Proceedings of the 17th Annual Conference of the Canadian Nuclear Society, CNS, Fredricton. 1996.

10. Fliscounakis, M., Girardi, E., Courau, T., 2011. A generalized pin-power reconstruction method for arbitrary heterogeneous geometries. In: M&C 2011, 8–12 May, Rio de Janero, Brasil.

11. Gomes, G. "Importance of Assembly Discontinuity Factors In Simulating Reactor Cores Containing Highly Heterogeneous Fuel Assemblies." Proc. of COMSOL Conference 2011.

12. Haroon, J., Kicka, L., Mohapatra, S., Nichita, E., and Schwanke, P. "Comparison of the Reactivity Effects Calculated by DRAGON and Serpent for a PHWR 37-element Fuel Bundle." Journal of Nuclear Engineering and Radiation Science.

13. Hebert, A. "A consistent technique for the pin-by-pin homogenization of a pressurized water reactor assembly." Nuclear Science and Engineering 113.3 (1993): 227-238.

14. Hebert, A. Applied reactor physics. Presses inter Polytechnique, 2009. 53

15. Hebert, A., “Development of the subgroup projection method for resonance self-shielding calculations,” Nuclear science and engineering, 162, 1, 56–75 (2009)

16. Hébert, A., Sekki, D., Chambon, R., 2014. A User Guide for DONJON Version5. Report IGE-344. École Polytechnique de Montréal.

17. Hebert, A “DRAGON5 and DONJON5, the contribution of École Polytechnique de Montréal to the SALOME platform,” Annals of Nuclear Energy, 87, Part 1, 12–20 (2016).

18. Hebert, A., “Development of the subgroup projection method for resonance self-shielding calculations,” Nuclear science and engineering, 162, 1, 56–75 (2009)

19. Hébert, A., Sekki, D., Chambon, R., 2014. A User Guide for DONJON Version5. Report IGE-344. École Polytechnique de Montréal.

20. Hébert, A., Sekki, D., Chambon, R., 2014. A User Guide for DONJON Version5. Report IGE-344. École Polytechnique de Montréal.

21. Herrero, J. J., García-Herranz, N., Cuervo, D., and Ahnert, C. "Neighborhood-corrected interface discontinuity factors for multi-group pin-by-pin diffusion calculations for LWR." Annals of Nuclear Energy 46 (2012): 106-115.

22. Hebert, A., and Santamarina, A., “Refinement of the Santamarina-Hfaiedh energy mesh between 22.5 eV and 11.4 keV” International Conference on Reactor Physics, Nuclear Power: A Sustainable Resource Casino-Kursaal Conference Center, Interlaken, Switzerland, September 14-19, 2008

23. Kim, H. R., and Cho, N. Z. "Global/local iterative methods for equivalent diffusion theory parameters in nodal calculation." Annals of Nuclear Energy 20.11 (1993): 767-783.

24. Marleau, G., Hébert, A., and Roy, R. "A User Guide for DRAGON, Release 3.05 E." Ecole Polytechnique de Montréal, Montréal, Canada (2009).

25. Marleau, G., Hébert, A., Roy, R., 2014. A USER GUIDE for DRAGON Version5. Report IGE-335. École Polytechnique de Montréal.

26. Merk, B., and Rohde, U. "An analytical solution for the consideration of the effect of adjacent fuel elements." Annals of Nuclear Energy 38.11 (2011): 2428-2440.

27. Nichita, E., and Rahnema, F. "A heterogeneous finite element method in diffusion theory." Annals of Nuclear Energy 30.3 (2003): 317-347.

28. Nichita, E., "Evaluating accuracy of standard homogenization and need for generalized equivalence theory for ACR®-lattice checkerboard configurations." Annals of Nuclear Energy 36.6 (2009): 760-766.

29. Rahnema, F. "Boundary condition perturbation theory for use in spatial homogenization methods." Nuclear Science and Engineering 102.2 (1989): 183-190.

30. Rahnema, F., and Nichita, E. M. "Leakage corrected spatial (assembly) homogenization technique." Annals of Nuclear Energy 24.6 (1997): 477-488.

31. Robinson, R. C., and Tran, F. "Calculation of homogenized Pickering NGS stainless steel adjuster rod neutron cross-sections

using conservation of reaction rates." 16 th Annual CNS conference, June 4 - 7, Saskaton, SK, Canada, 1995.

32. Santamarina, A., Collignon, C., and Garat,C., “French calculation schemes for light water reactor analysis,” The Physics of Fuel Cycles and Advanced Nuclear Systems: Global Developments (PHYSOR 2004) (2004)

33. Smith, K. S. “Spatial homogenization methods for light water reactor analysis.” Diss. Massachusetts Institute of Technology, 1980.

34. Smith, K. S. "Practical and efficient iterative method for LWR fuel assembly homogenization." Transactions of the American Nuclear Society71.CONF-941102-(1994).

35. Smith K., “Nodal diffusion methods: Understanding numerous unpublished details,” in “Proc. Int. Conf. PHYSOR,” (2016)

36. Shen, W. "Development of a multi-cell methodology to account for heterogeneous core effects in the core-analysis diffusion code." Proceeding of The International Conference on the Advances in Nuclear Analysis and Simulation, PHYSOR-2006, Vancouver, Canada. 2006.

37. Varin, E., Hébert, A., Roy, R., and Koclas, J. "A user guide for DONJON version 3.01." Ecole Polytechnique de Montréal, Montréal, Canada (2005).